

# Testing and Evaluation of Additively Manufactured TCR Core Materials<sup>‡</sup>

T.S. Byun<sup>\*</sup>, M.N. Gussev<sup>\*</sup>, B.E. Garrison<sup>\*</sup>, J. Simpson<sup>\*</sup>, M. Li<sup>†</sup>, X. Zhang<sup>†</sup>, K.A. Terrani<sup>\*</sup>

<sup>\*</sup>*Oak Ridge National Laboratory, 1 Bethel Valley Road, PO Box 2008, Oak Ridge, TN 37831*

<sup>†</sup>*Argonne National Laboratory, 9700 S Cass Ave, Lemont, IL 60439*

*byunts@ornl.gov*

*<https://dx.doi.org/10.13182/T122-32303>*

## INTRODUCTION

The Transformational Challenge Reactor (TCR) is a gas-cooled microreactor being developed to demonstrate a revolutionary approach to deploying new nuclear power systems [1,2]. One of the key transformational technologies employed in the TCR development program is fabrication of the core components using additive manufacturing (AM). As many AM technologies have matured to levels viable for fabrication of reactor components with complex shapes and varied functions, the vast majority of TCR core components, including SiC fuel blocks and metallic support structures, are to be fabricated using AM processes [3]. The AM technologies employed for fabrication of TCR core components initially included laser powder bed fusion (LPBF), and/or laser directed energy deposition (L-DED) for metallic components, and binder jetting combined with the chemical vapor infiltration (CVI) process for SiC components [3-5].

All of these printing processes consist of rapid melting-cooling cycles or swift binder jetting through a nozzle followed by CVI, in which appropriate process parameters need to be selected to tune and tailor material properties. Despite the tuning capabilities, the AM materials usually contain a high density of pores and other unique features in microstructure, which tend to result in unfavorable and significantly different properties when compared to those of the materials produced through traditional processing routes [3,6]. In this research, therefore, we aim to develop an integrated database for the mechanical and thermophysical properties and microstructural characteristics of the 3D-printed materials in support of reactor design and licensing activities and in order to provide feedback to the manufacturing processes.

## MATERIALS AND CHARACTERIZATION

Like other nuclear reactors, the TCR core is built with multiple materials, which include metallic internal structures supporting fuel blocks. The fuel form for the TCR consists of conventionally-fabricated UN TRISO fuel particles embedded inside a silicon carbide (SiC) matrix. The integrated fuel form is fabricated using binderjet printing of

SiC matrix followed by SiC chemical vapor infiltration [5]. In TCR these fuel blocks are stacked to form fuel columns and are supported by AM 316L structures. Except for the neutron moderator and its sheath – a wrought stainless-steel tube – the AM 316L and binder jet/CVI SiC are the primary non-fuel materials for the TCR core. Therefore, the testing and evaluation research focuses to produce mechanical properties and thermophysical data for those two materials before and after irradiation [3].

Mechanical testing for the AM 316L stainless steel will be performed to obtain engineering tensile properties (using SS-J2 specimens), creep properties (using standard and subsized specimens), high temperature burst properties, fracture and fatigue properties (using subsized specimens). Thermophysical properties such as specific heat, thermal conductivity and diffusivity, thermal expansion coefficient, and elastic constants are also measured using minidisk- and rod-shaped AM 316L specimens. The main mechanical properties for both the binder jet/CVI SiC and the reference CVD SiC will be the flexural strength [7] data from the 6 mm diameter disk specimens with different orientations. As an intermediate material, the green SiC (the printed and cured SiC before CVI) is also tested using various sizes of tensile specimens to examine the size effect on mechanical properties. The thermophysical properties of SiC will be also obtained from the disk or rod specimens.

In addition, SEM/TEM examination is carried out for the AM 316L steel in various conditions including stress-relieved and crept conditions. X-ray computed tomography (XCT) examination and in-situ deformation in SEM are also performed for investigating the mechanisms of deformation, fracture and creep.

## EXAMPLES OF RESULTS

The deformed and nondeformed microstructures of AM 316L stainless steel after creep testing at 650°C [3] are compared in Figure 1. Note that the nondeformed microstructure is obtained from the head of a tested creep specimen and is in an annealed condition (as it was tested at 650°C for ~15 hours). A relatively low density of pores is observed in this annealed AM 316L microstructure; however, a much higher density of pores is observed in the

<sup>‡</sup> This manuscript has been authored by UT-Battelle, LLC, under contract DE-AC05-00OR22725 with the US Department of Energy (DOE). The US government retains and the publisher, by accepting the article for publication, acknowledges that the US government retains a nonexclusive, paid-up, irrevocable, worldwide license to publish or reproduce the published form of this manuscript, or allow others to do so, for US government purposes. DOE will provide public access to these results of federally sponsored research in accordance with the DOE Public Access Plan (<http://energy.gov/downloads/doepublic-access-plan>).

crept microstructure (bottom photograph). This indicates that, although the pores formed in AM process can grow during creep testing, majority of the pores seen in the deformed microstructure are newly generated during the high temperature deformation and failure process.

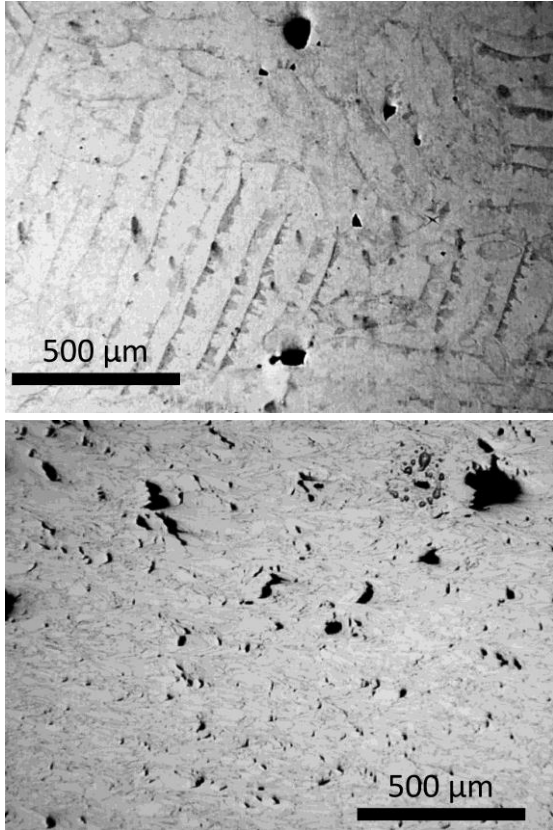


Figure 1. Microstructures of nondeformed (top) and deformed (bottom) AM 316L after creep testing at 650°C/225MPa.

The tensile stress-strain curves of AM 316L and reference (or wrought) 316L stainless steels are compared in Figure 2. At room temperature (25°C) the AM 316L steel shows higher initial strength and total elongation than the reference 316L steel. This might be due to the unique microstructure of AM 316L steel, which usually contains strong residual stress fields and dislocation networks etc. A hardened microstructure of austenitic stainless steels usually shows more linear slip behavior and hence sustainable work hardening, which led to a higher elongation at room temperature. At 300°C, however, the characteristic linear slip is reduced, and the initial high strength cannot be sustained by further hardening. In the AM 316L steel the lower hardening rate in the high strain range ends up with lower maximum strength and lower ductility, when compared to the wrought counterpart.

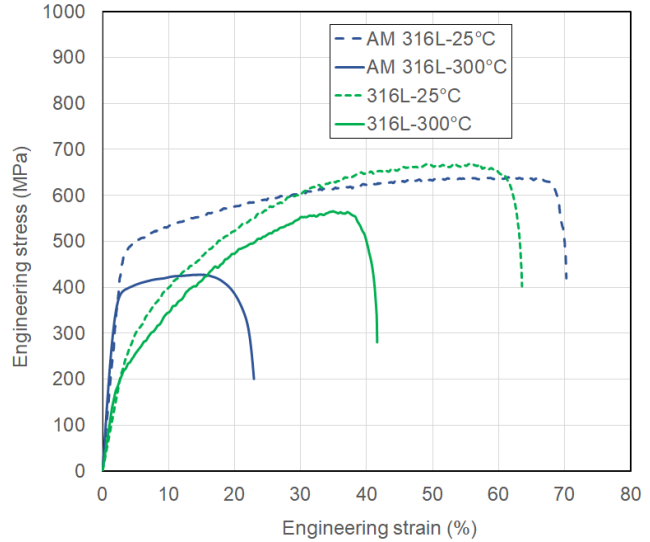


Figure 2. Comparison of engineering stress-strain curves for the AM 316L and wrought 316L steels. Specimens were loaded in their weaker (i.e., Z and T) directions.

The next dataset is from the tensile specimens printed by binder jetting and curing heat treatment (SiC green material). Uniaxial tensile testing for the large (gage section 225 mm<sup>3</sup>) and small or mini (6 mm<sup>3</sup>) as-printed (green) SiC specimens has been performed and the failure data (UTS) are plotted for Weibull statistics in Figure 3. This is to investigate the effects of specimen size and printer parameter (nozzle distance for the new and old) on strength. Figure 3 indicates that smaller (mini) specimens are stronger but show generally lower Weibull modulus, which is a general size effect. It is also noted that the smaller specimens in the x-direction from the old printer are weaker than their larger counterparts, which might be because of the coarser nozzle movement.

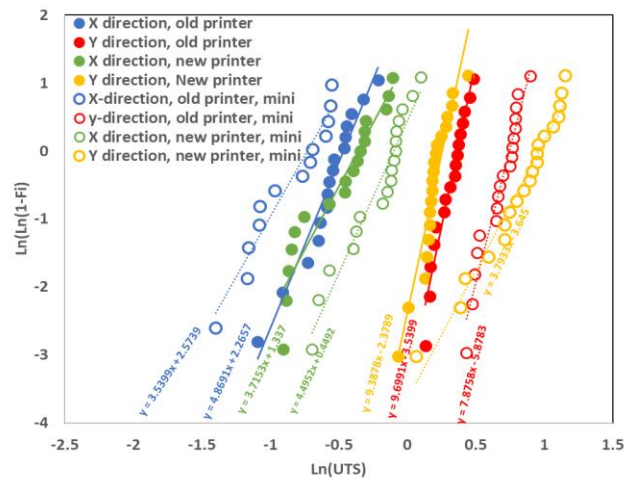


Figure 3. Weibull plots of the uniaxial tensile failure data of green SiC specimens with different sizes.

Figure 3 also shows that the Weibull moduli evaluated for the green (as-printed) SiC specimens are in the range of 3.5 – 9.7. The SiC specimens are also tested after the final CVI process. Our preliminary results for the CVI-SiC specimens indicate that they have similar or higher moduli, 7 – 10, when compared to those in green condition. Meanwhile, a stark difference is found in their failure strength: the failure strength of the CVI SiC specimens is approximately two orders of magnitude higher than those of the as-printed SiC specimens.

## CONCLUDING REMARKS

The additive manufacturing technology has been matured to apply to fabrication of complex reactor components, including core internals of the gas-cooled microreactor TCR. Although the mechanical property data produced up to date are limited, it may be concluded based on the expert knowledge of materials microstructure and radiation effects that the performance of the AM materials are not inferior to the traditionally processed materials. A comprehensive set of thermophysical properties and microstructure characterization data, including those after irradiation, is expected to be available in the coming years.

## ACKNOWLEDGEMENT

This research was supported by the Transformational Challenge Reactor program supported by the US Department of Energy, Office of Nuclear Energy.

## REFERENCES

1. Oak Ridge National Laboratory. "Transformational Challenge Reactor." Oak Ridge National Laboratory. <https://tcr.ornl.gov/>
2. B. J. Ade et al., "Candidate Core Designs for the Transformational Challenge Reactor," presented at the PHYSOR 2020 – Transition to a Scalable Nuclear Future, Cambridge, United Kingdom, 2020.
3. K.G. Field et al., "Handbook of advanced manufactured material properties from TCR structure builds at ORNL – FY19," ORNL/TM-2019/1328, Oak Ridge National Laboratory (2019).
4. J. Simpson, J. Haley, C. Cramer, O. Shafer, A. Elliot, W. Peter, L. Love, R. Dehoff, "Considerations for application of additive manufacturing to nuclear reactor core components," ORNL/TM-2019-1190, Oak Ridge National Laboratory (2019).
5. K. Terrani, B. Jolly, M. Trammell, "3D printing of high-purity silicon carbide," *Journal of the American Ceramic Society* 103 (2020), 1575-1581.
6. T.M. Mower, M.J. Long, "Mechanical Behavior of Additive Manufactured Powder-bed Laser-Fused materials" *Materials Science and Engineering: A*, 651 (2016) 198-213.

7. S. Kondo, Y. Katoh, L.L. Snead, Concentric ring on ring test for unirradiated and irradiated miniature SiC specimens, *J. Nucl. Mater.* 417 (2011) 406–410.